Rheol. Acta **19**, 404 – 420 (1980)

ISSN 0035-4511 / ASTM-Coden: RHEAAK

Department of Aerospace Engineering and Mechanics, University of Minnesota, Minneapolis, Minnesota (USA)

The stick-slip problem for a round jet
I. Large surface tension

S. A. Trogdon and *D. D. Joseph*

With 12 figures and 3 tables

(Received January 31, 1980)

1. Introduction

A jet of fluid is extruded from a round pipe at low speed with gravity and wind shear neglected. The fluid must adjust from a fully developed flow in the pipe to a uniform flow far downstream. At low speeds this adjustment appears to require that the jet swell, and the swelling is much larger in viscoelastic fluids than in Newtonian ones. The swelling is called die swell or extrudate swell. There is no analytical solution of the die swell problem when the nonlinear terms are important although it appears to be possible to calculate the swell in the Newtonian case by numerical methods: *Nickell, Caswell,* and *Tanner* (11); *Chang, Patten,* and *Finlayson* (2); *Silliman* and *Scriven* (16); *Omodei* (13). Numerical methods have also been used in the non-Newtonian case: *Tanner* and *Reddy* (18); *Chang, Patten,* and *Finlayson* (2), but the results are less satisfactory since convergence can only be obtained for fluids with a small elastic component. A different numerical method, with convergence proofs, has recently been presented by *Jean* and *Pritchard* (7) for a problem related to die swell.

Richardson (14) used the Wiener-Hopf method to solve the stick-slip problem for Stokes flow of a plane jet of a Newtonian fluid extruded from a two-dimensional channel. In this stick-slip problem the fluid is thought to be confined to an infinite strip of fixed height. One half of the strip, $-\infty < x \leq 0$ is bounded by rigid walls at $y = \pm a$ and the fluid is pushed through this strip by a prescribed pressure gradient at $x \to -\infty$. The fluid which leaves the channel $x = 0$ is also confined to a plane channel with the same boundaries at $y = \pm a$. The fluid sticks to the channel wall at $y = \pm a, x < 0$ and it slips at the channel wall when $x > 0$. Having once obtained the solution of this problem the shape of the free surface ($x > 0$) may be computed by requiring that the shape of the free surface is such as to balance the jump in the normal stress at each point of the boundary of the jet. The computational algorithm can be regarded as arising from perturbing a strip of motionless fluid with a slow flow (see *Joseph* (8)).

Sturges (17) solved the same stick-slip problem, and got the same solution as *Richardson*, by expanding the solution in the jet as a Fourier series, the solution in the channel as a biorthogonal series, matching the velocity and stresses on the common boundary $x = 0$ where the jet meets the channel. Previously, *Zidan* (21) had applied this method of matching but he did not obtain the correct solution because his set of eigenfunctions in the jet were not complete (they do not contain the terms proportional to x, see our eq. [3.30]).

In this paper we solve the stick-slip problem for a round jet. The round jet is very important for applications and experiments. We solve the problem by the Wiener-Hopf method used by *Richardson* and by the eigenfunction method used by *Sturges* for the plane jet. The eigenfunction method is much easier to implement than the Wiener-Hopf method. The results obtained by the two methods agree. Our solution, then, is completely reliable. We have given graphs of the interesting quantities: velocities, stresses, pressure and the shape of the free surface.

2. Equations governing the "stick-slip" problem

We imagine a cylinder of radius $\hat{r} = a$ where generators extend from $\hat{x} = -\infty$ to $\hat{x} = \infty$. The plane $\hat{x} = 0$ separates the fluid filled pipe, $\hat{x} < 0$, from the jet, $\hat{x} > 0$. The fluid sticks to the pipe and the shear stress vanishes on the jet (see fig. 1). The linearized mathematical problem can be viewed as arising from a perturbation of the rest state in which the

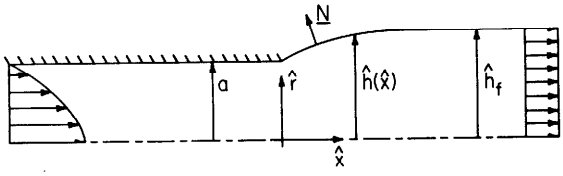

Fig. 1a. The capillary jet

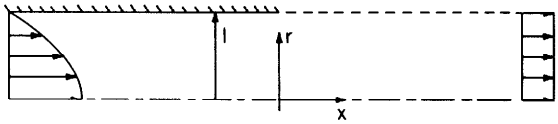

Fig. 1b. The domain of the rest state for the capillary jet

motionless jet is held together in a cylinder of radius a by surface tension; *Joseph* (8). The perturbation parameter is $\varepsilon = Q/2\pi$ where

$$Q = 2\pi \int_0^{\hat{h}(\hat{x})} \boldsymbol{e}_x \cdot \hat{\boldsymbol{u}}(\hat{x},r;\varepsilon) r\,dr$$

is the volume flux. We are interested in determining the stream function of the motion $\hat{\psi}(\hat{x},\hat{r})$ and the jet shape $\hat{h}(\hat{x})$ when ε is small. We seek these fields in terms of dimensionless variables

$$(x,r) = \frac{1}{a}(\hat{x},\hat{r}),$$

$$\hat{\psi}(\hat{x},\hat{r}) = \varepsilon\psi(x,r),$$

$$\hat{\Phi}(\hat{x},\hat{r}) = \frac{\sigma}{a} + \frac{\varepsilon}{a^3}\Phi(x,r),$$

and

$$\hat{h}(\hat{x}) = a[1 + \varepsilon h(x)].$$

The problem satisfied by ψ and h is summarized below:

$$\mathscr{L}^2\psi = 0$$

in the pipe and in the jet,

$$\mathscr{L} \overset{\text{def}}{=} r\frac{\partial}{\partial r}\left(\frac{1}{r}\frac{\partial}{\partial r}\right) + \frac{\partial^2}{\partial x^2} \qquad [2.1]$$

where ψ is the stream function for axisymmetric flow,

$$\boldsymbol{u} = \operatorname{curl}\left(\boldsymbol{e}_\theta \frac{\psi}{r}\right) \qquad [2.2]_1$$

is the velocity,

$$u = \frac{1}{r}\frac{\partial\psi}{\partial r} \qquad [2.2]_2$$

is the axial (x) component of velocity and

$$w = -\frac{1}{r}\frac{\partial\psi}{\partial x} \qquad [2.2]_3$$

is the radial (r) component of velocity. The cylinder $r = 1$ is a streamline

$$\psi(x,1) = 1, \quad -\infty < x < \infty. \qquad [2.3]$$

Since $\boldsymbol{u} = 0$ on the wall of the pipe,

$$\frac{\partial\psi(x,1)}{\partial r} = 0, \quad -\infty < x \le 0. \qquad [2.4]$$

The vanishing of the shear stress on the free surface of the jet may be expressed as

$$\frac{\partial}{\partial r}\left(\frac{1}{r}\frac{\partial\psi}{\partial r}\right) = 0, \quad 0 \le x < \infty. \qquad [2.5]$$

The flow far downstream ($x \to -\infty$) is assumed to be independent of x; that is

$$\psi \to r^2(2 - r^2) \quad \text{as} \quad x \to -\infty. \qquad [2.6]$$

Far upstream ($x \to \infty$) the flow is uniform,

$$Q = 2\pi \int_0^{\hat{h}_f} \hat{U}_\infty r\,dr = \pi\hat{h}_f^2\hat{U}_\infty = 2\pi\varepsilon.$$

Hence

$$\hat{U}_\infty = \frac{2\varepsilon}{\hat{h}_f^2}.$$

Using

$$\hat{U}_\infty = \frac{\varepsilon}{a^2}U_\infty \quad \text{and} \quad \hat{h}_f = a[1 + \varepsilon h_f]$$

we find that

$$U_\infty = 2.$$

Hence

$$\frac{1}{r}\frac{\partial\psi}{\partial r} \to 2 \quad \text{as} \quad x \to \infty. \qquad [2.7]$$

The problem [2.1] to [2.7] is well set and possesses a solution $\psi(x,r)$, apparently unique, which we shall construct. After finding $\psi(x,r)$ we may compute the pressure by integrating the equation of motion

$$-\operatorname{grad}\Phi + \operatorname{div}\boldsymbol{S} = 0 \qquad [2.8]$$

where $\Phi = p - p_a$ is the reduced pressure for zero body force and $\boldsymbol{S} = \mu[\operatorname{grad}\boldsymbol{u} + (\operatorname{grad}\boldsymbol{u})^T]$ is the deviatoric stress. The stresses are related to the stream function as follows

$$S\langle rr\rangle = 2\mu\frac{\partial}{\partial r}\left(\frac{1}{r}\frac{\partial\psi}{\partial x}\right),$$

$$S\langle rx\rangle = \mu\left[\frac{\partial}{\partial r}\left(\frac{1}{r}\frac{\partial\psi}{\partial r}\right) - \frac{1}{r}\frac{\partial^2\psi}{\partial x^2}\right],$$

$$S\langle\theta\theta\rangle = \frac{-2\mu}{r^2}\frac{\partial\psi}{\partial x},$$

$$S\langle xx\rangle = \frac{2\mu}{r}\frac{\partial^2\psi}{\partial r\partial x}.$$

Finally we note that so far we have not imposed any condition of continuity for the normal stress at the jet surface. Such a condition is necessary in order to relate the unknown jet shape to the field quantities. The usual assumption is that the jump in normal stress at the jet surface is balanced by surface tension times the mean curvature of the surface. Symbolically this may be expressed as

$$[-\hat{\Phi}\mathbf{1} + \hat{\mathbf{S}}]\boldsymbol{n}\cdot\boldsymbol{n} = -\frac{\sigma}{\hat{h}\hat{h}'}\frac{d}{d\hat{x}}\left[\frac{\hat{h}}{(1+\hat{h}'^2)^{1/2}}\right],$$

$$\hat{h}' \overset{\text{def}}{=} \frac{d\hat{h}}{d\hat{x}}$$

on $\hat{r} = \hat{h}(\hat{x})$, or, in the context of the linearized problem [2.1] to [2.7], in dimensionless variables

$$-\frac{2\mu}{r}\frac{\partial^2\psi}{\partial r\partial x} - \Phi = a^2\sigma[h'' + h], \quad h'' \overset{\text{def}}{=} \frac{d^2h}{dx^2} \qquad [2.9]$$

on $r = 1$.

Given ψ and Φ we may solve [2.9] relative to two point boundary conditions. We take $h'(x) \to 0$ as $x \to \infty$ and note that the solution is not determined until, for example, some condition on $h(x)$ for $x = 0$ is specified. For example we could specify $h(0)$ or $h'(0)$ or a linear combination of these two. As $x \to \infty$, $\Phi \to \Phi_+$, a constant, and [2.9] reduces to

$$\Phi_+ = -a^2\sigma\lim_{x\to\infty} h. \qquad [2.10]$$

The swell of the die may now be defined by $h_f = \lim_{x\to\infty} h(x)$, the jet swells when $h_f > 0$ and contracts when $h_f < 0$. It is obvious that h_f is a functional of the solution of [2.9] which depends on the conditions on h imposed at $x = 0$. We will suppose that the liquid separates from the jet at a sharp edge; that is,

$$h(0) = 0. \qquad [2.11]$$

3. Wiener-Hopf Solution for the stream function

Now we shall solve the problem posed in §2 by the method of *Wiener* and *Hopf*. Our analysis is inspired by the work of *Richardson* (14) in which he applies the method to the problem of the *plane* jet extruded from flow between plane walls. Though our analysis is for the round jet we can, nevertheless, economize on the writing by following closely and in sequence the analysis given by *Richardson* in the plane case.

The analysis of the exit lip singularity in the plane problem should apply in the round one. Near a singularity we expect that second derivatives will be much larger than first derivatives and $\mathscr{L}^2 \to \nabla^4$ near the singularity. So the analysis at the exit lip is locally plane and the results of *Michael* (10) and *Richardson* (14) apply: ψ tends to zero like the 3/2 power of the distance from the exit lip. This means that the stresses are singular there with a characteristic square root singularity.

To apply the method of *Wiener* and *Hopf* we temporarily replace condition [2.3] with

$$\psi(x,1) = e^{-\varepsilon|x|}, \quad \varepsilon > 0 \qquad [3.1]$$

and, after determining the solution, we let $\varepsilon \to 0$. We define the Fourier transform pair

$$\Psi(\omega,r) = \int_{-\infty}^{\infty}\psi(x,r)e^{i\omega x}dx,$$

$$\psi(x,r) = \frac{1}{2\pi}\int_{-\infty}^{\infty}\Psi(\omega,r)e^{-ix\omega}d\omega. \qquad [3.2]$$

The condition [3.1] is necessary to guarantee that the first integral is bounded. Taking transforms of $\mathscr{L}^2\psi = 0$ and [3.1] we find that $\Psi(\omega,r)$ satisfies

$$L^2\Psi = 0, \quad L = r\frac{d}{dr}\left(\frac{1}{r}\frac{d}{dr}\right) - \omega^2 \qquad [3.3]$$

and

$$\Psi(\omega,1) = \frac{2\varepsilon}{\omega^2 + \varepsilon^2}. \qquad [3.4]$$

The solutions of [3.3] which are bounded at $r = 0$ are in the form

$$\Psi(\omega,r) = C_1 r I_1(\omega r) + C_2 r^2 I_0(\omega r) \qquad [3.5]$$

where [3.5] will satisfy [3.4] if C_1, C_2 are chosen so that

$$\Psi(\omega,r) = A(\omega)\left[\frac{rI_1(\omega r)}{I_1(\omega)} - \frac{r^2 I_0(\omega)}{I_0(\omega)}\right] + \frac{2\varepsilon}{\omega^2+\varepsilon^2} r\frac{I_1(\omega r)}{I_1(\omega)}. \quad [3.6]$$

To accommodate the remaining boundary condition [2.4] and [2.5] we need expressions for the derivatives:

$$\frac{\partial\Psi(\omega\, r)}{\partial r} \overset{\text{def}}{=} \Psi^{(1)}(\omega,r) = A(\omega)\left[\frac{\omega r I_0(\omega r)}{I_1(\omega)} - \frac{2rI_0(\omega r)+\omega r^2 I_1(\omega r)}{I_0(\omega)}\right] + \frac{2\varepsilon}{\omega^2+\varepsilon^2}\left[\frac{\omega r I_0(\omega r)}{I_1(\omega)}\right], \quad [3.7]$$

$$\frac{\partial^2\Psi}{\partial r^2} \overset{\text{def}}{=} \Psi^{(2)}(\omega,r) = A(\omega)\left[\frac{\omega I_0(\omega r)+\omega^2 r I_1(\omega r)}{I_1(\omega)} - \frac{2I_0(\omega r)+3\omega r I_1(\omega r)+\omega^2 r^2 I_0(\omega r)}{I_0(\omega)}\right], \quad [3.8]$$

$$\Psi^{(2,1)}(\omega,1) \overset{\text{def}}{=} \Psi^{(2)}(\omega,1) - \Psi^{(1)}(\omega,1). \quad [3.9]$$

We next write $\Psi(\omega,r)$ as the sum of two parts, $\Psi_+(\omega,r)$ and $\Psi_-(\omega,r)$ where

$$\Psi_+(\omega,r) = \int_0^\infty \psi(x,r)e^{i\omega x}dx,$$

$$\Psi_-(\omega,r) = \int_{-\infty}^0 \psi(x,r)e^{i\omega x}dx \quad [3.10]$$

and $\Psi_+(\omega,r)$ is analytic in ω for $\mathrm{Im}(\omega) > -\varepsilon$ and $\Psi_-(\omega,r)$ is analytic for $\mathrm{Im}(\omega) < \varepsilon$ (Noble (12), Theorem A). These conditions come necessarily from the transform of $e^{-\varepsilon|x|}$. We then see that $\Psi(\omega,r)$ is regular in the strip $-\varepsilon < \mathrm{Im}(\omega) < \varepsilon$. Transforming conditions [2.4] and [2.5] we get

$$\Psi_-^{(1)}(\omega,1) = 0, \quad [3.11]$$

$$\Psi_+^{(2,1)}(\omega,1) = 0. \quad [3.12]$$

Noting next that

$$\Psi^{(1)}(\omega,1) = \Psi_-^{(1)}(\omega,1) + \Psi_+^{(1)}(\omega,1)$$

and

$$\Psi^{(2,1)}(\omega,1) = \Psi_-^{(2,1)}(\omega,1) + \Psi_+^{(2,1)}(\omega,1)$$

where $\Psi^{(1)}(\omega,1)$ and $\Psi^{(2,1)}(\omega,1)$ are given by [3.7] through [3.9] we find that

$$\Psi_+^{(1)}(\omega,1) = A(\omega)\left[\frac{\omega I_0(\omega)}{I_1(\omega)} - \frac{\omega I_1(\omega)}{I_0(\omega)} - 2\right] + \frac{2\varepsilon}{\omega^2+\varepsilon^2}\left[\frac{\omega I_0(\omega)}{I_1(\omega)}\right] \quad [3.13]$$

and

$$\Psi_-^{(2,1)}(\omega,1) = -A(\omega)\left[\frac{2\omega I_1(\omega)}{I_0(\omega)}\right] + \frac{2\varepsilon}{\omega^2+\varepsilon^2}\omega^2. \quad [3.14]$$

Eliminating $A(\omega)$ from [3.13] and [3.14], we find that

$$\Psi_+^{(1)}(\omega,1) + B(\omega)\Psi_-^{(2,1)}(\omega,1) = \frac{\omega^2\varepsilon}{\omega^2+\varepsilon^2}\cdot\left[\frac{I_0^2(\omega) - I_1^2(\omega)}{I_1^2(\omega)}\right]$$

where

$$B(\omega) = \frac{1}{2}\left[\frac{\omega I_0^2(\omega) - 2I_0(\omega)I_1(\omega) - \omega I_1^2(\omega)}{\omega I_1^2(\omega)}\right]. \quad [3.16]$$

Eq. [3.15] is the type of equation dealt with by the method of *Wiener* and *Hopf*. To implement the method we must first effect the decomposition, $B(\omega) = B_+(\omega)B_-(\omega)$ where $B_+(\omega)$ is regular and non-zero for $\mathrm{Im}(\omega) > -\varepsilon$ and $B_-(\omega)$ is regular and non-zero for $\mathrm{Im}(\omega) < \varepsilon$.

We write eq. [3.16] as

$$B(\omega) = \frac{F_1(\omega)}{[F_2(\omega)]^2}$$

where

$$F_1(\omega) = \frac{1}{2}\left[\frac{\omega I_0^2(\omega) - 2I_0(\omega)I_1(\omega) - \omega I_1^2(\omega)}{\omega^3}\right]$$

and

$$F_2(\omega) = \frac{I_1(\omega)}{\omega}.$$

Both $F_1(\omega)$ and $F_2(\omega)$ are integral functions of ω with only simple poles and neither are zero at $\omega = 0$; in fact, $\lim_{\omega\to 0} F_1(\omega) = 1/2$ and $\lim_{\omega\to 0} F_2(\omega) = -1/16$. Thus, the required decomposition can be effected by using the infinite product theorem for integral functions.

The product representation for $F_2(\omega)$ is given by

$$\frac{I_1(\omega)}{\omega} = \frac{1}{2}\prod_{n=1}^{\infty}\left(1 - \frac{\omega}{iq_n}\right)\left(1 + \frac{\omega}{iq_n}\right)$$

where iq_n are the zeros of $I_1(\omega)$ in the upper half plane, and the product representation for $F_1(\omega)$ is given by

$$\frac{1}{2}\left[\frac{\omega I_0^2(\omega) - 2I_0(\omega)I_1(\omega) - \omega I_1^2(\omega)}{\omega^3}\right] = -\frac{1}{16}\prod_{n=1}^{\infty}\left(1 + \frac{\omega}{\omega_n}\right)\left(1 - \frac{\omega}{\omega_n}\right) \cdot \left(1 + \frac{\omega}{\bar{\omega}_n}\right)\left(1 - \frac{\omega}{\bar{\omega}_n}\right),$$

where ω_n are the first quadrant zeros of

$$\omega I_0^2(\omega) - 2I_0(\omega)I_1(\omega) - \omega I_1^2(\omega).$$

We note for future use that if iq_n are the zeros of $I_1(\omega)$ in the upper half plane, then q_n are the zeros of $J_1(q)$ in the right half plane; and if ω_n are the first quadrant zeros of

$$\omega I_0^2(\omega) - 2I_0(\omega)I_1(\omega) - \omega I_1^2(\omega)$$

then $p_n = i\bar{\omega}_n$ are the first quadrant zeros of

$$pJ_0^2(p) - 2J_0(p)J_1(p) + pJ_1^2(p).$$

The zeros of $J_1(q)$ in the right half plane are given asymptotically by *Abromowitz* and *Stegun* (1) as

$$q_n \sim \frac{\pi}{2}\left(2n + \frac{1}{2}\right) - \frac{3}{4\pi(2n + \frac{1}{2})}, \quad n = 1,2,3,... \qquad [3.17]$$

and the first quadrant zeros of

$$pJ_0^2(p) - 2J_0(p)J_1(p) + pJ_1^2(p) \stackrel{\text{def}}{=} F(p)$$

are given asymptotically by *Trogdon* (20) as

$$p_n = Z_n^0 + \delta_n \qquad [3.18]$$

where

$$2Z_n^0 = (\xi_n - \eta_n) + i\left(\log 2\xi_n + \frac{\eta_n^2}{2}\right),$$

$$\xi_n = (2n + 1)\pi, \quad \eta_n = \frac{\log 2\xi_n}{\xi_n},$$

and

$$\delta_n = -\frac{F(Z_n^0)}{F'(Z_n^0)}, \quad n = 1,2,3,... .$$

The required factorization of $B(\omega)$ can now be effected where,

$$B_+(\omega) = -\frac{1}{4}\prod_{n=1}^{\infty}\frac{\left(1 + \frac{\omega}{\omega_n}\right)\left(1 - \frac{\omega}{\bar{\omega}_n}\right)}{\left(1 + \frac{\omega}{iq_n}\right)^2} \qquad [3.19]$$

and

$$B_-(\omega) = \prod_{n=1}^{\infty}\frac{\left(1 - \frac{\omega}{\omega_n}\right)\left(1 + \frac{\omega}{\bar{\omega}_n}\right)}{\left(1 - \frac{\omega}{iq_n}\right)^2} = -4B_+(-\omega). \qquad [3.20]$$

We note that $B_+(\omega)$ is analytic and non-zero for Im $(\omega) > -q_1$ and $B_-(\omega)$ is analytic and non-zero for Im $(\omega) < q_1$. With the use of [3.17] and [3.18] $B_\pm(\omega)$ can be shown to be absolutely an uniformly convergent, and $B_\pm(\omega)$ behaves like $\omega^{-1/2}$ as $|\omega| \to \infty$. Even though the products converge absolutely and uniformly, their convergence is extremely slow, the n^{th} term in the products behaving like

$$1 \mp \frac{\omega/2\pi i}{(n + \frac{1}{2})(n + \frac{1}{4})}$$

for large n. Hence from the outset one sees that if the products are to be used in computations, some numerical artifice[1]) must be employed to compute them.

Eq. [3.15] may now be written as

$$\frac{\Psi_+^{(1)}(\omega,1)}{B_+(\omega)} + B_-(\omega)\Psi_-^{(2,1)}(\omega,1) = C(\omega) \qquad [3.21]$$

where

$$C(\omega) = \frac{\omega^2\varepsilon}{B_+(\omega)(\omega^2 + \varepsilon^2)}\left[\frac{I_0^2(\omega) - I_1^2(\omega)}{I_1^2(\omega)}\right].$$

Next we must effect the decomposition

$$C(\omega) = C_+(\omega) + C_-(\omega)$$

[1]) Proof of convergence of the products is dependent upon obtaining a function which behaves asymptotically like the products (see Noble, 1958). Such a function can be obtained by using the asymptotic form of the "eigenvalues", i.e., eqs. [3.17] and [3.18]. The numerical artifice mentioned above consists in using enough terms in the infinite products such that after some truncation number, say N, the asymptotic function may be used for computations. The asymptotic function can then be employed to estimate the contribution of the remaining terms. This method proved extremely effective, with considerable savings in computational time.

where

$C_+(\omega)$ is regular for $\mathrm{Im}(\omega) > -\varepsilon$

and

$C_-(\omega)$ is regular for $\mathrm{Im}(\omega) < \varepsilon$.

The singularities of $C(\omega)$ are as follows:

(i) simple poles at $\omega = \pm i\varepsilon$,
(ii) simple poles at $\omega = -\omega_n$ and $\bar{\omega}_n$, $n = 1,2,3,\ldots$,
(iii) double poles at $\omega = \pm iq_n$, $n = 1,2,3,\ldots$.

The decomposition of $C(\omega)$ can be effected by considering the integral

$$I_k(\omega) = \frac{1}{2\pi i}\int_{\Gamma_k} \frac{C(t)}{t-\omega}\,dt,$$

where Γ_k is an appropriate sequence of contours in the t-plane such that as $k \to \infty$, Γ_k encloses all the poles of $C(t)/(t-\omega)$. From the behavior of $C(t)$ for large $|t|$, $I_k(\omega) \to 0$ as $k \to \infty$. Thus, in the limit, $I_k(\omega)$ is equal to the sum of the residues at all the poles of $C(t)/(t-\omega)$ in the plane. Hence,

$$C(\omega) = -\Sigma\,\mathrm{Residues}\left[\frac{C(t)}{t-\omega}\right]_{t\neq\omega}$$

in the plane. Thus we find that

$$C_+(\omega) = \frac{1}{\omega + i\varepsilon}\frac{i\varepsilon^2}{2B_+(-i\varepsilon)}\left[\frac{J_0^2(\varepsilon)+J_1^2(\varepsilon)}{J_1^2(\varepsilon)}\right] + \text{terms that tend to zero as } \varepsilon \to 0, \qquad [3.22]$$

and

$$C_-(\omega) = -\frac{1}{\omega - i\varepsilon}\frac{i\varepsilon^2}{2B_+(i\varepsilon)}\left[\frac{J_0^2(\varepsilon)+J_1^2(\varepsilon)}{J_1^2(\varepsilon)}\right] + \text{terms that tend to zero as } \varepsilon \to 0. \qquad [3.23]$$

Eq. [3.21] may now be written as

$$\frac{\Psi_+^{(1)}(\omega,1)}{B_+(\omega)} + B_-(\omega)\Psi_-^{(2,1)}(\omega,1) = C_+(\omega) + C_-(\omega)$$

or, upon rearranging

$$\frac{\Psi_+^{(1)}(\omega,1)}{B_+(\omega)} - C_+(\omega) = C_-(\omega) - B_-(\omega)\Psi_-^{(2,1)}(\omega) \equiv H(\omega). \qquad [3.24]$$

The left-hand side of [3.24] is analytic for $\mathrm{Im}(\omega) > -\varepsilon$ and the right-hand side is analytic for $\mathrm{Im}(\omega) < \varepsilon$, which implies that $H(\omega)$ is analytic in the entire ω-plane.

In order to determine $H(\omega)$ we must make asymptotic estimates of $\Psi_+^{(1)}(\omega,1)$ and $\Psi_-^{(2,1)}(\omega,1)$ as $|\omega| \to \infty$. These estimates can be obtained if we know the behavior of

$$\left.\frac{\partial\psi}{\partial r}\right|_{r=1} \quad \text{as} \quad x \to 0^+$$

and

$$\left.\frac{\partial^2\psi}{\partial r^2} - \frac{1}{r}\frac{\partial\psi}{\partial r}\right|_{r=1} \quad \text{as} \quad x \to 0^-.$$

Locally, at $x = 0$, we assume that results for the plane jet are applicable, and following *Richardson* we obtain

$$\left.\frac{\partial\psi}{\partial r}\right|_{r=1} \sim x^{1/2} \quad \text{as} \quad x \to 0^+,$$

$$\left.\frac{\partial^2\psi}{\partial r^2} - \frac{1}{r}\frac{\partial\psi}{\partial r}\right|_{r=1} \sim x^{-1/2} \quad \text{as} \quad x \to 0^-.$$

Using the usual methods for asymptotic estimates of Fourier integrals, e.g. *Titchmarsh* (19), we find that

$\Psi_+^{(1)}(\omega,1) \to \omega^{-3/2}$ as $|\omega| \to \infty$ in the upper half plane

and

$\Psi_-^{(2,1)}(\omega,1) \to \omega^{-1/2}$ as $|\omega| \to \infty$ in the lower half plane.

Hence, it follows from [3.24] that $H(\omega) = o(1)$, so that by *Liouville's* theorem $H(\omega) \equiv 0$. Thus [3.24] gives,

$$\Psi_+^{(1)}(\omega,1) = B_+(\omega)C_+(\omega) \qquad [3.25]$$

and

$$\Psi_-^{(2,1)}(\omega,1) = \frac{C_-(\omega)}{B_-(\omega)}.$$

Substituting [3.25] into [3.13] and [3.14] we find $A(\omega)$ in the form,

$$A(\omega) = \frac{\varepsilon}{\omega^2+\varepsilon^2}\frac{\omega I_0(\omega)}{I_1(\omega)} - \frac{I_0(\omega)}{2\omega I_1(\omega)}\frac{C_-(\omega)}{B_-(\omega)} \qquad [3.26]_1$$

or

$$A(\omega) = -\frac{2\varepsilon}{\omega^2+\varepsilon_2}\cdot\left[\frac{\omega I_0^2(\omega)}{\omega I_0^2(\omega) - 2I_0(\omega)I_1(\omega) - \omega I_1^2(\omega)}\right] + \frac{I_1(\omega)I_0(\omega)B_+(\omega)C_+(\omega)}{\omega I_0^2(\omega) - 2I_0(\omega)I_1(\omega) - \omega I_1^2(\omega)}. \qquad [3.26]_2$$

The two eqs. [3.26] are of course identical and each will prove useful in what follows.

Substituting [3.26] into [3.6] we obtain,

$$\Psi(\omega,r) = \frac{\varepsilon}{\omega^2+\varepsilon^2}\frac{\omega I_0(\omega)}{I_1(\omega)} \cdot \left[\frac{rI_1(\omega r)}{I_1(\omega)} - \frac{r^2 I_0(\omega r)}{I_0(\omega)}\right] - \frac{I_0(\omega)}{2\omega I_1(\omega)}\frac{C_-(\omega)}{B_-(\omega)} \cdot \left[\frac{rI_1(\omega r)}{I_1(\omega)} - \frac{r^2 I_0(\omega r)}{I_0(\omega)}\right] + \frac{2\varepsilon}{\omega^2+\varepsilon^2}\frac{rI_1(\omega r)}{I_1(\omega)} \qquad [3.27]_1$$

or

$$\Psi(\omega,r) = -\frac{2\varepsilon}{\omega^2+\varepsilon^2} \cdot \frac{\omega I_0^2(\omega)}{\omega I_0^2(\omega) - 2I_0(\omega)I_1(\omega) - \omega I_1^2(\omega)} \cdot \left[\frac{rI_1(\omega r)}{I_1(\omega)} - \frac{r^2 I_0(\omega r)}{I_0(\omega)}\right] + \frac{I_1(\omega)I_0(\omega)B_+(\omega)C_+(\omega)}{\omega I_0^2(\omega) - 2I_0(\omega)I_1(\omega) - \omega I_1^2(\omega)} \cdot \left[\frac{rI_1(\omega r)}{I_1(\omega)} - \frac{r^2 I_0(\omega r)}{I_0(\omega)}\right] + \frac{2\varepsilon}{\omega^2+\varepsilon^2}\frac{rI_1(\omega r)}{I_1(\omega)}. \qquad [3.27]_2$$

The following observation is useful for inverting [3.27]: $C_-(\omega)/B_-(\omega)$ is analytic in the lower half plane and $B_+(\omega)C_+(\omega)$ is analytic in the upper half plane. The inversion integral $[3.21]_2$ may now be evaluated. When $x > 0$ we use $[3.27]_1$ and complete a contour in the lower half plane find that,

$$\psi(x,r) = -i\{\Sigma \text{ Residues of } \Psi(\omega,r)e^{-ix\omega} \text{ in the lower half plane}\}.$$

When $x < 0$ we use $[3.27]_2$ and complete a contour in the upper half plane to find that,

$$\psi(x,r) = i\{\Sigma \text{ Residues of } \Psi(\omega,r)e^{-ix\omega} \text{ in the upper half plane}\}.$$

Thus, upon taking $\lim_{\varepsilon\to 0}$ and noting that $\lim_{\varepsilon\to 0} B_+(\pm i\varepsilon) = -1/4$ and hence that $\lim_{\varepsilon\to 0} C_\pm(\omega) = \mp 8i/\omega$; we find that for $x > 0$,

$$\psi(x,r) = r^2 - 4\sum_1^\infty \frac{1}{q_n^2 B_-(-iq_n)} \cdot \frac{rJ_1(q_n r)}{J_0(q_n)} x e^{-q_n x} + 4\sum_1^\infty \lim_{\omega\to -iq_n}\frac{d}{d\omega}\left[\frac{i}{\omega^2 B_-(\omega)}\right] \cdot \frac{rJ_1(q_n r)}{J_0(q_n)} e^{-q_n x} \qquad [3.28]$$

and for $x < 0$,

$$\psi(x,r) = r^2(2-r^2) + 8\,\mathrm{Re}\left\{\sum_1^\infty \frac{B_+(ip_n)}{p_n J_1^2(p_n)} \cdot [rJ_0(p_n)J_1(p_n r) - r^2 J_1(p_n)J_0(p_n r)]e^{p_n x}\right\}. \qquad [3.29]$$

It will be convenient for comparing the Wiener-Hopf result just obtained with the to-be-derived results from the matching of biorthogonal series, to define

$$A_n = \frac{4}{J_0(q_n)}\lim_{\omega\to -iq_n}\frac{d}{d\omega}\left[\frac{i}{\omega^2 B_-(\omega)}\right],$$

$$B_n = -\frac{4}{q_n^2 J_0(q_n)B_-(-iq_n)}$$

and

$$C_n = \frac{4B_+(ip_n)}{p_n J_n^2(p_n)}.$$

In terms of these coefficients we have

$$\psi(x,r) = r^2 + \sum_1^\infty (A_n + B_n x)e^{-q_n x} rJ_1(q_n r) \quad \text{for } x > 0, \qquad [3.30]$$

and

$$\psi(x,r) = r^2(2-r^2) + \sum_{-\infty}^{\infty} C_n e^{p_n x}[rJ_0(p_n)J_1(p_n r) - r^2 J_1(p_n)J_0(p_n r)] \quad \text{for } x < 0, \qquad [3.31]$$

where $C_{-n} = \bar{C}_n$ and $p_{-n} = \bar{p}_n$.

The required field quantities may now be found by differentiation of [3.30] and [3.31].

4. The pressure and the shape of the free surface

The pressure is found as a solution to the equation,

$$-\operatorname{grad}\Phi + \mu V^2 \boldsymbol{u} = 0,$$

where $\boldsymbol{u}$ is given by $\boldsymbol{u} = \operatorname{curl}\left(e_\theta \frac{\psi}{r}\right)$.

Thus, we find that

$$\Phi(x,r) = 2\mu \sum_1^\infty q_n B_n e^{-q_n x} J_0(q_n r) + \Phi_+ \qquad [4.1]$$

for $x > 0$ and

$$\Phi(x,r) = -16\mu x + 2\mu \sum_{-\infty}^{\infty} C_n p_n J_1(p_n) e^{p_n x} J_0(p_n r) + \Phi_- \qquad [4.2]$$

for $x < 0$ where Φ_+ and Φ_- are constants to be determined from the conditions that $\Phi_+ = \lim_{x\to\infty} \Phi(x,r) = -\sigma a^2 h_f$ and $\Phi(x,r)$ is continuous at $x = 0$. It follows that

$$2\mu \sum_{-\infty}^{\infty} C_n p_n J_1(p_n) J_0(p_n r) + \Phi_- = 2\mu \sum_1^\infty q_n B_n J_0(q_n r) - \sigma a^2 h_f .$$

Multiplying this by r and integrating from 0 to 1 we find that

$$\Phi_- = -4\mu \sum_{-\infty}^{\infty} C_n J_1^2(p_n) - \sigma a^2 h_f , \qquad [4.3]$$

where $h_f = \lim_{x\to\infty} h(x)$ is still to be determined from the solution of the equations governing $h(x)$. At this stage we may compute

$$-4 \sum_{-\infty}^{\infty} C_n J_1^2(p_n) \sim 3.55 .$$

The shape of the free surface is governed by the following differential equation,

$$a^2\sigma(h'' + h) = -\frac{2\mu}{r} \frac{\partial^2 \psi(x,1)}{\partial r \partial x} - \Phi(x,1) \qquad [4.4]$$

subject to the boundary conditions

$$h(0) = 0, \quad h'(\infty) = 0. \qquad [4.5]$$

Upon substituting [3.30] and [4.1] into [4.4] we obtain

$$h'' + h = \frac{2\mu}{a^2\sigma} \sum_1^\infty [q_n(A_n + B_n x) - 2B_n] \cdot e^{-q_n x} J_0(q_n) + h_f . \qquad [4.6]$$

The solution to [4.6] subject to conditions [4.5] is a particular integral of [4.6]. Thus

$$h(x) = \frac{2\mu}{a^2\sigma} \sum_1^\infty [(a_n + b_n x) e^{-q_n x} - a_n] J_0(q_n) \qquad [4.7]$$

where,

$$a_n = \frac{q_n[q_n A_n + 2(b_n - B_n)]}{1 + q_n^2},$$

$$b_n = \frac{q_n^2}{1 + q_n^2} B_n .$$

After evaluating [4.7] as $x \to \infty, h \to h_f$ we find that

$$h_f = -\frac{2\mu}{a^2\sigma} \sum_1^\infty a_n J_0(q_n) = \frac{\mu}{a^2\sigma}(.494). \qquad [4.8]$$

It then follows from [4.3] that the constant part of the pressure is given by

$$\Phi_- = (3.06)\mu .$$

The swell of the round jet in dimensional variables may be obtained from [4.8] as

$$\frac{\hat{h}_f}{a} = 1 + \frac{\mu \bar{U}}{\sigma}(.247) + o(\varepsilon) \qquad [4.9]$$

where $\bar{U} = Q/\pi a^2$ is the average velocity in the pipe. This formula may be compared with *Richardson's* (14) expression for the swell of the plane jet

$$\frac{\hat{h}_f}{a} = 1 + \frac{\mu \bar{U}}{\sigma}(.356) + o(\varepsilon) \qquad [4.10]$$

where a is one half of the channel height and $\bar{U}$ is the average velocity in the channel.

5. The method of matched eigenfunction expansions

We now forget about the method of Wiener-Hopf and proceed by expanding the solution in the jet into Fourier series and the solution in the pipe into biorthogonal series. These representations give the solution in terms of the eigenfunctions "natural" to different regions. For the method to be succesful it is necessary that the eigenfunction bases used be complete with respect to expansions of arbitrary functions. In the present case we may take [3.30] as the expansion appropriate for the jet and [3.31] as the expansion appropriate for the pipe. In fourth-order problems the right bases are very dependent on boundary conditions. The bases eigenfunctions should satisfy the boundary

conditions. The completeness question is crucial. We already noted in the Introduction that *Zidan* (21) tried the method of this section but was not successful because he left out the term proportional to x in [3.30]. The expansion [3.31] is proved to be complete by *Joseph* (9) and *Gregory* (5).

The coefficients in [3.30] and [3.31] are at present unknown. They are to be determined by matching. The matching leads to the Wiener-Hopf coefficients used in [3.28] and [3.29] but in a special superior way which we will discuss after we specify the algorithm used for the computation of the coefficients A_n, B_n and C_n in [3.30] and [3.31].

To determine these coefficients we follow *Sturges* (17) in requiring that the *velocity and stress fields be pointwise continuous at each value r in the exit plane* $x = 0$. Matching velocities requires that

$$\psi(0^-,r) = \psi(0^+,r), \qquad [5.1]$$

$$\frac{\partial\psi(0^-,r)}{\partial x} = \frac{\partial\psi(0^+,r)}{\partial x}. \qquad [5.2]$$

Assuming now that [5.1] and [5.2] are satisfied identically in r we can match the stresses across the exit plane if

$$\frac{\partial^2\psi(0^-,r)}{\partial x^2} = \frac{\partial^2\psi(0^+,r)}{\partial x^2} \qquad [5.3]$$

and

$$\Phi(0^-,r) = \Phi(0^+,r). \qquad [5.4]$$

To convert [5.4] into an equation for ψ we solve the eqs. [2.8] for $\partial\Phi/\partial r$. Then $\partial\Phi/\partial r$ is continuous across $x = 0$ if

$$\frac{\partial^3\psi(0^-,r)}{\partial x^3} = \frac{\partial^3\psi(0^+,r)}{\partial x^3}. \qquad [5.5]$$

The conditions [5.1] through [5.5] evidently determine the coefficients A_n, B_n and C_n uniquely by a truncation, plus iteration procedure of a familiar kind.

Substituting [3.30] and [3.31] into [5.1 – 5.4] we get

$$\sum_{-\infty}^{\infty} C_n[rJ_0(p_n)J_1(p_nr) - r^2J_1(p_n)J_0(p_nr)] + r^2(1-r^2) = \sum_{1}^{\infty} A_m r J_1(q_m r), \qquad [5.6]$$

$$\sum_{-\infty}^{\infty} C_n p_n[rJ_0(p_n)J_1(p_nr) - r^2J_1(p_n)J_0(p_nr)] = \sum_{1}^{\infty}(B_m - p_m A_m) r J_1(q_m r), \qquad [5.7]$$

$$\sum_{-\infty}^{\infty} C_n p_n^2[rJ_0(p_n)J_1(p_nr) - r^2J_1(p_n)J_0(p_nr)] = \sum_{1}^{\infty} q_m(q_m A_m - 2B_m) r J_1(q_m r), \qquad [5.8]$$

$$\sum_{-\infty}^{\infty} C_n p_n^3[rJ_0(p_n)J_1(p_nr) - r^2J_1(p_n)J_0(p_nr)] = \sum_{1}^{\infty} q_m^2(3B_m - q_m A_m) r J_1(q_m r). \qquad [5.9]$$

In order to obtain expressions for the coefficients we make use of the orthogonality property of Bessel functions. Multiplying the above by $J_1(q_k r)$ and integrating from 0 to 1 we obtain the following equations for the coefficients.

$$\sum_{-\infty}^{\infty} S_{mn} C_n + G_m = A_m f_m, \qquad [5.10]$$

$$\sum_{-\infty}^{\infty} S_{mn} C_n p_n = (B_m - q_m A_m) f_m, \qquad [5.11]$$

$$\sum_{-\infty}^{\infty} S_{mn} C_n p_n^2 = q_m(q_m A_m - 2B_m) f_m, \qquad [5.12]$$

$$\sum_{-\infty}^{\infty} S_{mn} C_n p_n^3 = q_m^2(3B_m - q_m A_m) f_m \qquad [5.13]$$

where,

$$S_{mn} = \int_0^1 [rJ_0(p_n)J_1(p_nr) - r^2J_1(p_n)J_0(p_nr)] \cdot J_1(q_m r)dr = \frac{2q_m p_n J_0(q_m)J_1^2(p_n)}{(p_n^2 - q_m^2)^2},$$

$$G_m = \int_0^1 r^2(1-r^2)J_1(q_m r)dr = \frac{-8}{q_m^3} J_0(q_m),$$

and

$$f_m = \int_0^1 r J_1^2(q_m r)dr = \frac{1}{2} J_0^2(q_m).$$

Solving [5.10] and [5.12] for A_m and B_m we obtain,

$$A_m = \frac{1}{f_m}\sum_{-\infty}^{\infty} S_{mn} C_n + \frac{G_m}{f_m}, \qquad [5.14]$$

$$B_m = \frac{1}{2f_m}\sum_{-\infty}^{\infty} S_{mn} C_n\left[q_m - \frac{p_n^2}{q_m}\right] + \frac{q_m G_m}{2f_m}, \qquad [5.15]$$

and solving [5.11] and [5.13] for A_m and B_m we obtain,

$$A_m = \frac{1}{2f_m}\sum_{-\infty}^{\infty} S_{mn} C_n \left[\frac{p_n^3}{q_m^3} - \frac{3p_n}{q_m}\right], \qquad [5.16]$$

$$B_m = \frac{1}{2f_m}\sum_{-\infty}^{\infty} S_{mn} C_n \left[\frac{p_n^3}{q_m^2} - p_n\right]. \qquad [5.17]$$

By equating [5.14] to [5.16] and [5.15] to [5.17] we obtain the following system of equations,

$$\sum_{-\infty}^{\infty} S_{mn} C_n \left[\frac{p_n^3}{2q_m^3} - \frac{3p_n}{2q_m^3} - 1\right] = G_m \qquad [5.18]$$

and,

$$\sum_{-\infty}^{\infty} S_{mn} C_n \left[\frac{p_n^3}{q_m^3} + \frac{p_n^2}{q_m^2} - \frac{p_n}{q_m} - 1\right] = G_m. \qquad [5.19]$$

Eqs. [5.18] and [5.19] are an infinite set of equations for the coefficients C_n. To solve these equations we replace the infinite sum-

Table 1. Convergence of the coefficients $A_n^{(N)}$ and $B_n^{(N)}$ to the coefficients A_n and B_n as a function of the truncation number N

n	$A_n^{(10)}$	$A_n^{(20)}$	$A_n^{(50)}$	$A_n^{(100)}$	A_n
1	.48134E + 00	.48770E + 00	.49153E + 00	.49279E + 00	.49402E + 00
2	−.12372E + 00	−.12669E + 00	−.12847E + 00	−.12904E + 00	−.12960E + 00
3	.54655E − 01	.56555E − 01	.57708E − 01	.58079E − 01	.58436E − 01
4	−.30321E − 01	−.31703E − 01	−.32554E − 01	−.32828E − 01	−.33089E − 01
5	.19087E − 01	.20159E − 01	.20834E − 01	.21052E − 01	.21258E − 01
6	−.13024E − 01	−.13890E − 01	−.14447E − 01	−.14628E − 01	−.14798E − 01
7	.93990E − 02	.10117E − 01	.10591E − 01	.10746E − 01	.10891E − 01
8	−.70684E − 02	−.76759E − 02	−.80867E − 02	−.82220E − 02	−.83487E − 02
9	.54868E − 02	.60085E − 02	.63701E − 02	.64904E − 02	.66028E − 02
10	−.43675E − 02	−.48210E − 02	−.51430E − 02	−.52512E − 02	−.53523E − 02
11		.39464E − 02	.42358E − 02	.43342E − 02	.44262E − 02
12		−.32845E − 02	−.35466E − 02	−.36368E − 02	−.37211E − 02
13		.27720E − 02	.30109E − 02	.30941E − 02	.31720E − 02
14		−.23676E − 02	−.25865E − 02	−.26637E − 02	−.27360E − 02
15		.20431E − 02	.22446E − 02	.23166E − 02	.23842E − 02
16		−.17789E − 02	−.19652E − 02	−.20326E − 02	−.20960E − 02
17		.15613E − 02	.17341E − 02	.17974E − 02	.18571E − 02
18		−.13799E − 02	−.15407E − 02	−.16004E − 02	−.16569E − 02
19		.12273E − 02	.13774E − 02	.14338E − 02	.14873E − 02
20		−.10978E − 02	−.12382E − 02	−.12916E − 02	−.13426E − 02

n	$B_n^{(10)}$	$B_n^{(20)}$	$B_n^{(50)}$	$B_n^{(100)}$	B_n
1	.10703E + 01	.11010E + 01	.11211E + 01	.11280E + 01	.11350E + 01
2	−.51148E + 00	−.53682E + 00	−.55432E + 00	−.56052E + 00	−.56684E + 00
3	.32717E + 00	.34945E + 00	.36554E + 00	.37140E + 00	.37746E + 00
4	−.23625E + 00	−.25628E + 00	−.27135E + 00	−.27698E + 00	−.28288E + 00
5	.18248E + 00	.20071E + 00	.21495E + 00	.22040E + 00	.22619E + 00
6	−.14718E + 00	−.16391E + 00	−.17743E + 00	−.18272E + 00	−.18842E + 00
7	.12235E + 00	.13779E + 00	.15068E + 00	.15583E + 00	.16146E + 00
8	−.10401E + 00	−.11834E + 00	−.13066E + 00	−.13568E + 00	−.14125E + 00
9	.89972E − 01	.10332E + 00	.11512E + 00	.12003E + 00	.12554E + 00
10	−.78911E − 01	−.91395E − 01	−.10271E + 00	−.10751E + 00	−.11297E + 00
11		.81710E − 01	.92584E − 01	.97280E − 01	.10269E + 00
12		−.73700E − 01	−.84163E − 01	−.88761E − 01	−.94122E − 01
13		.66975E − 01	.77055E − 01	.81559E − 01	.86875E − 01
14		−.61255E − 01	−.70977E − 01	−.75391E − 01	−.80665E − 01
15		.56337E − 01	.65722E − 01	.70051E − 01	.75283E − 01
16		−.52066E − 01	−.61136E − 01	−.65382E − 01	−.70574E − 01
17		.48328E − 01	.57101E − 01	.61267E − 01	.66420E − 01
18		−.45030E − 01	−.53523E − 01	−.57612E − 01	−.62727E − 01
19		.42103E − 01	.50330E − 01	.54345E − 01	.59424E − 01
20		−.39488E − 01	−.47465E − 01	−.51408E − 01	−.56451E − 01

mation with a finite one $\sum_{-N}^{N}$. Then we compute $2N$ approximate coefficients $C_n^{(N)}$. The coefficients and [5.16] and [5.17] then determine the truncated approximating coefficients $A_n^{(N)}$ and $B_n^{(N)}$. We examine convergence by increasing the truncation number N. Choosing the coefficients $C_n^{(N)}$ as typical, we except in general that

$$|C_n^{(N)} - C_n^{(M)}| \to 0, \quad N > M \to \infty . \qquad [5.20]$$

In fact, our numerical work shows that this is true for each fixed $|n| < M$, $M \to \infty$. In the present case we can assume that the coefficients given by Wiener-Hopf are exact so that, in addition to [5.20], we can examine the convergence of the approximate coefficients $C_n^{(N)}$ to the exact ones $|C_n - C_n^{(N)}|$ for large N.

Tables 1 and 2 give the numerical values which show convergence of $A_n^{(N)}$, $B_n^{(N)}$ and $C_n^{(N)}$ with the truncation number N.

Table 2. Convergence of the coefficients $C_n^{(N)}$ to the coefficients C_n as a function of the truncation number N. $C_n = (\mathrm{Re}[C_n], \mathrm{Im}[C_n])$

n	$C_n^{(10)}$	$C_n^{(20)}$	$C_n^{(50)}$
1	(.66215E − 01, .20552E + 00)	(.66558E − 01, .19655E + 00)	(.66581E − 01, .19154E + 00)
2	(.22887E − 01, .10519E + 00)	(.23274E − 01, .97116E − 01)	(.23283E − 01, .92944E − 01)
3	(.11040E − 01, .70039E − 01)	(.11569E − 01, .61991E − 01)	(.11596E − 01, .58187E − 01)
4	(.60393E − 02, .53146E − 01)	(.67852E − 02, .44658E − 01)	(.68326E − 02, .41042E − 01)
5	(.32988E − 02, .43977E − 01)	(.43849E − 02, .34605E − 01)	(.44541E − 02, .31078E − 01)
6	(.13470E − 02, .39026E − 01)	(.30156E − 02, .28183E − 01)	(.31073E − 02, .24677E − 01)
7	(−.64346E − 03, .37072E − 01)	(.21598E − 02, .23812E − 01)	(.22763E − 02, .20275E − 01)
8	(−.38927E − 02, .38136E − 01)	(.15853E − 02, .20709E − 01)	(.17302E − 02, .17094E − 01)
9	(−.12793E − 01, .43193E − 01)	(.11746E − 02, .18446E − 01)	(.13534E − 02, .14706E − 01)
10	(−.48555E − 01, .37827E − 01)	(.86253E − 03, .16776E − 01)	(.10834E − 02, .12860E − 01)
11		(.60864E − 03, .15549E − 01)	(.68374E − 03, .11398E − 01)
12		(.38445E − 03, .14678E − 01)	(.73219E − 03, .10218E − 01)
13		(.16519E − 03, .14115E − 01)	(.61461E − 03, .92485E − 02)
14		(−.77756E − 04, .13849E − 01)	(.52164E − 03, .84418E − 02)
15		(−.38888E − 03, .13909E − 01)	(.44690E − 03, .77624E − 02)
16		(−.85689E − 03, .14384E − 01)	(.38592E − 03, .71845E − 02)
17		(−.17011E − 02, .15475E − 01)	(.33551E − 03, .66886E − 02)
18		(−.36044E − 02, .17595E − 01)	(.29333E − 03, .62600E − 02)
19		(−.93569E − 02, .21111E − 01)	(.25764E − 03, .58872E − 02)
20		(−.28883E − 01, .14672E − 01)	(.22712E − 03, .55612E − 02)

n	$C_n^{(100)}$	C_n
1	(.66564E − 01, .18995E + 00)	(.66536E − 01, .18642E + 00)
2	(.23261E − 01, .91666E − 01)	(.23229E − 01, .90453E − 01)
3	(.11577E − 01, .57063E − 01)	(.11550E − 01, .56015E − 01)
4	(.68191E − 02, .40016E − 01)	(.67964E − 02, .39075E − 01)
5	(.44441E − 02, .30119E − 01)	(.44251E − 02, .29255E − 01)
6	(.31004E − 02, .23768E − 01)	(.30843E − 02, .22961E − 01)
7	(.22719E − 02, .19402E − 01)	(.22581E − 02, .18642E − 01)
8	(.17279E − 02, .16249E − 01)	(.17160E − 02, .15526E − 01)
9	(.13530E − 02, .13883E − 01)	(.13427E − 02, .13192E − 01)
10	(.10846E − 02, .12053E − 01)	(.10756E − 02, .11388E − 01)
11	(.88466E − 03, .10604E − 01)	(.87852E − 03, .99618E − 02)
12	(.73630E − 03, .94318E − 02)	(.72930E − 03, .88100E − 02)
13	(.62004E − 03, .84686E − 02)	(.61384E − 03, .78642E − 02)
14	(.52833E − 03, .76653E − 02)	(.52285E − 03, .70762E − 02)
15	(.45484E − 03, .69871E − 02)	(.44997E − 03, .64116E − 02)
16	(.39510E − 03, .64082E − 02)	(.39079E − 03, .58448E − 02)
17	(.34594E − 03, .59094E − 02)	(.34213E − 03, .53569E − 02)
18	(.30505E − 03, .54760E − 02)	(.30168E − 03, .49333E − 02)
19	(.27070E − 03, .50966E − 02)	(.26774E − 03, .45627E − 02)
20	(.24158E − 03, .47622E − 02)	(.23899E − 03, .42363E − 02)

Now we shall make an interesting remark about convergence. *It is frequently better to compute the solution using all the 2 N approximate coefficients of a given approximation of 2N terms than to use 2N of the exact coefficients as an approximation of 2N terms.* In fact, as in a *Weierstrass* approximation the approximate coefficients are chosen to give a best fit to the data and another choice of $2N$ coefficients, even choosing the exact ones, will give a less good approximation.

This interesting feature of convergence can be exhibited for the constant part

$$\phi \overset{\text{def}}{=} \frac{\Phi_- + \sigma a^2 h_f}{\mu} = -4 \sum_{-\infty}^{\infty} C_n J_1^2(p_n) \qquad [5.21]$$

of the pressure (see [4.3]). Let

$$\phi^{(N)} = -4 \sum_{-N}^{N} C_n^{(N)} J_1^2(p_n) \qquad [5.22]$$

be the approximation after truncation. Convergence to ϕ on the right side of [5.21] is slow. In Appendix I we show that ϕ converges like $(n + \frac{1}{2})^{-3/2}$ and table 3 shows that $\phi^{(100)} = 3.53$ whereas

$$\phi = -4 \sum_{-100}^{100} C_n J_1^2(p_n) = 3.15 . \qquad [5.23]$$

It is shown in Appendix II that

$$3.552 < \phi < 3.554 ,$$

hence the approximate solution [5.22] of 100 terms is better than the 100 term approximation [5.23] of the exact solution. The difference between these two approximations is less important when convergence is more rapid, as in the case of the final radius of the free surface

$$H_f \overset{\text{def}}{=} \frac{h_f}{\mu/\sigma a^2} = -2 \sum_{1}^{\infty} a_n J_0(q_n) , \qquad [5.24]$$

$$H_f^{(N)} = -2 \sum_{1}^{\infty} a_n^{(N)} J_0(q_n) .$$

Table 3. Convergence of the constant part of the pressure and the final radius

N	10	20	50	100	
$\phi^{(N)}$	3.29	3.42	3.50	3.53	$-4 \sum_{-100}^{100} C_n J_1^2(p_n) = 3.15$
$H_f^{(N)}$	.467	.481	.489	.492	$-2 \sum_{1}^{100} a_n J_0(q_n) = .494$

6. Results and discussion

In figures 2 through 12 we have plotted velocity, stress, pressure and the shape of the free surface for slow flow. The extra stresses (except $S\langle\theta\theta\rangle$ and pressure have a square root singularity at $x = 0, r = 1$. The singularity of the pressure and the radial stress subtract out, leaving a finite radial part $T\langle rr\rangle = -\Phi + S\langle rr\rangle$; for a discussion of this point, see *Richardson* (14).

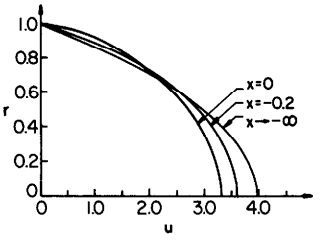

Fig. 2a. Axial component of velocity in the pipe

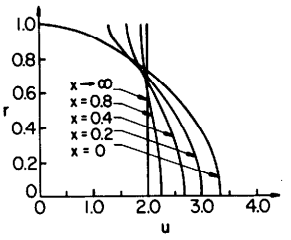

Fig. 2b. Axial component of velocity in the jet

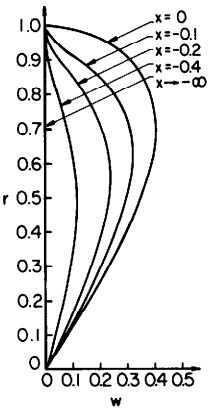

Fig. 3a. Radial component of velocity in the pipe

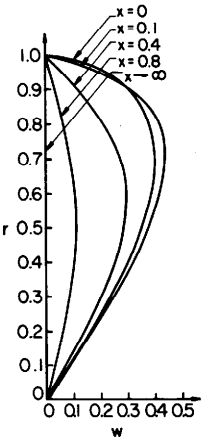

Fig. 3b. Radial component of velocity in the jet

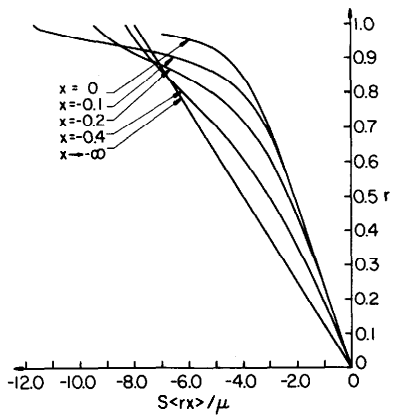

Fig. 4a. Shear stress distribution in the pipe

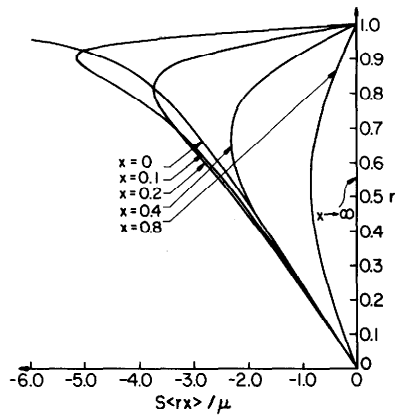

Fig. 4b. Shear stress distribution in the jet

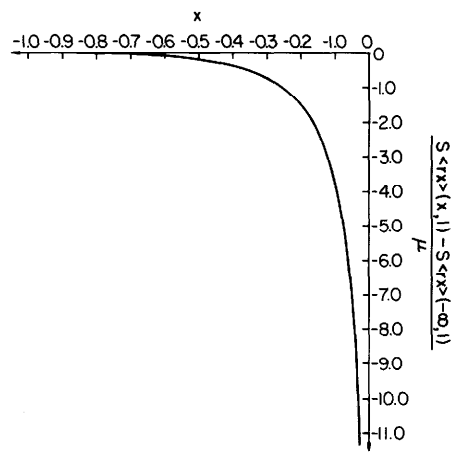

Fig. 5. Shear stress discrepancy at the boundary $r = 1$ of the pipe

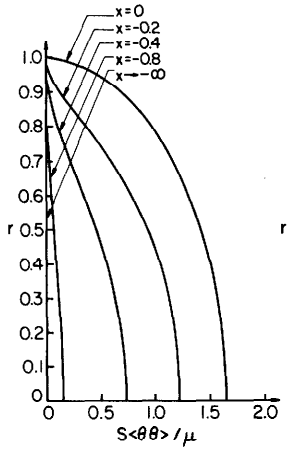

Fig. 6a. Hoop stress distribution in the pipe

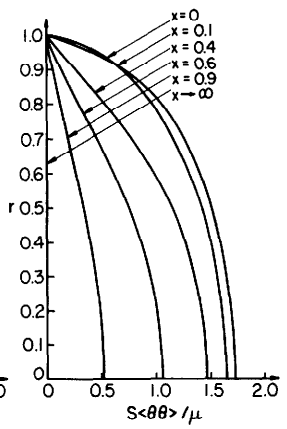

Fig. 6b. Hoop stress distribution in the jet

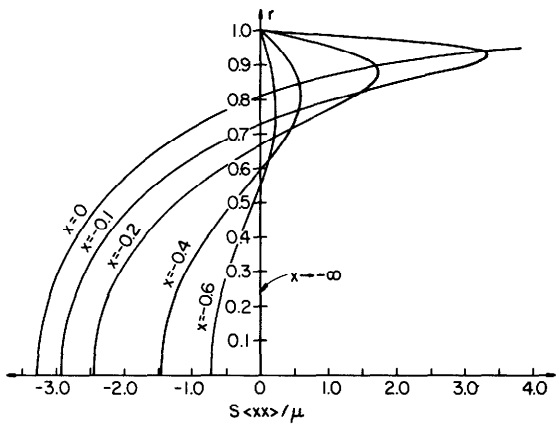

Fig. 7a. Axial extra stress distribution in the pipe

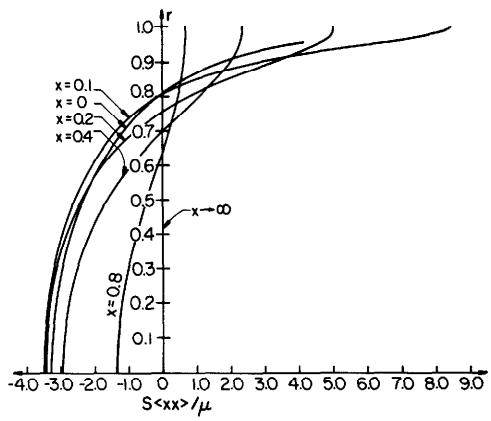

Fig. 7b. Axial extra stress distribution in the jet

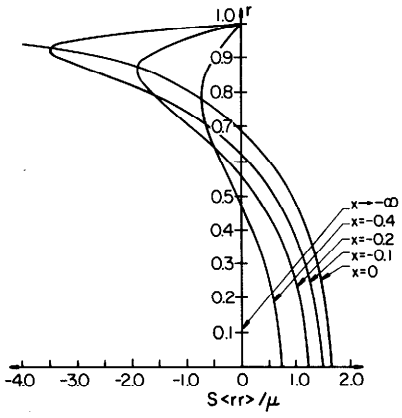

Fig. 8a. Radial extra stress distribution in the pipe

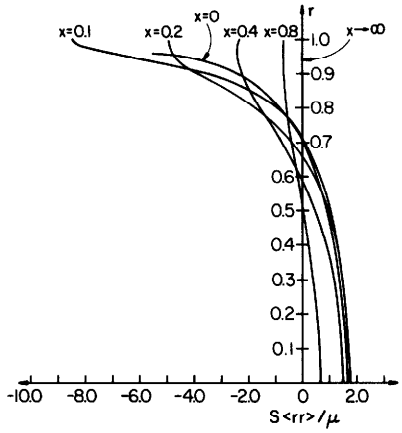

Fig. 8b. Radial extra stress distribution in the jet

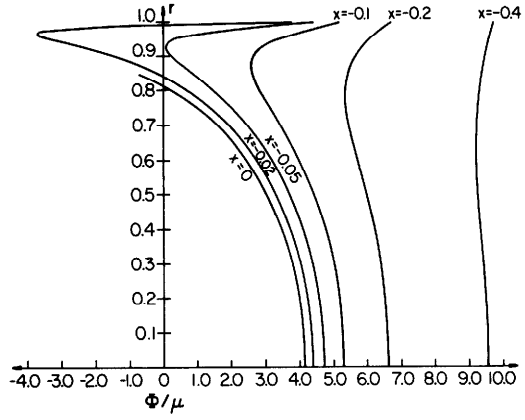

Fig. 9a. The pressure distribution in the pipe

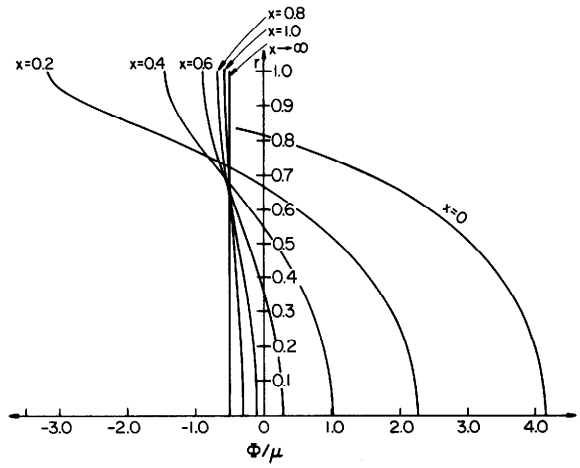

Fig. 9b. The pressure distribution in the jet

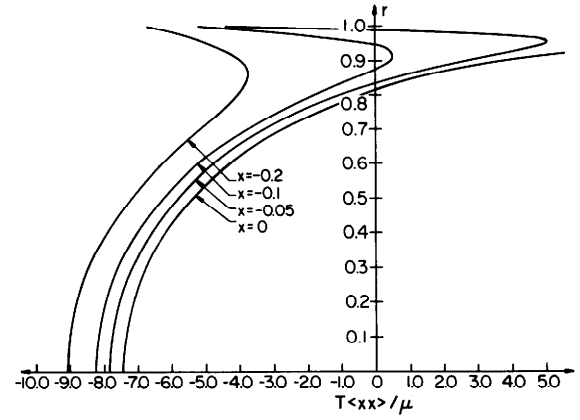

Fig. 10a. The total axial stress distribution in the pipe

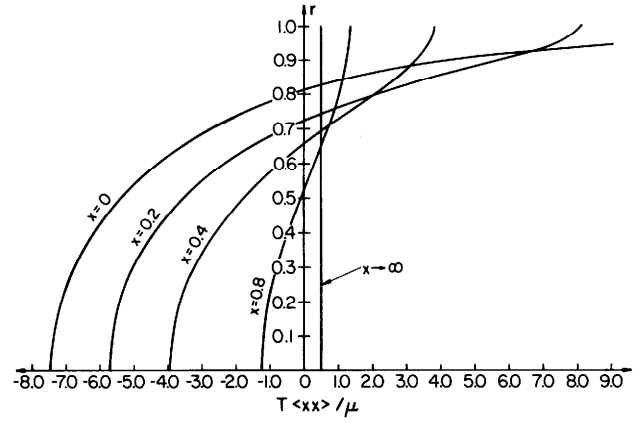

Fig. 10b. The total axial stress distribution in the jet

The basic dynamics of the jet are reflected in the velocity adjustments shown in figures 2 and 3. These adjustments take a pipe flow, which is close to parabolic in the pipe into a plug flow far downstream in the jet. The plug flow has no shear stresses at the boundary of the jet and is otherwise a solution of the governing equations. So we expect that the outer

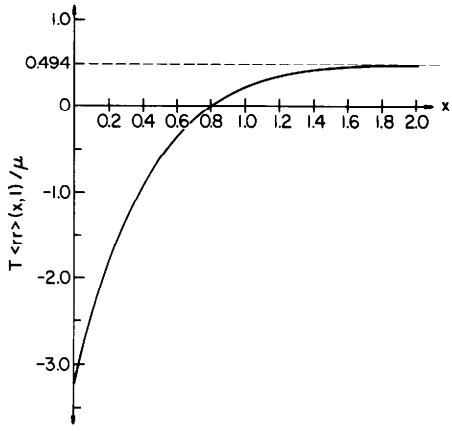

Fig. 11. The radial stress at the boundary of the jet

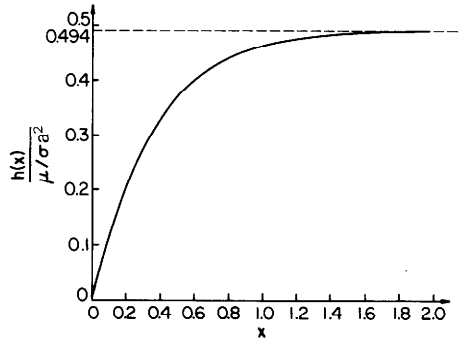

Fig. 12. Correction coefficient for the shape of the free surface

layers of the fluid in the jet will speed up and the inner layers will slow down when the jet leaves the pipe. This type of dynamics is certainly characteristic of the solutions exhibited here and in the numerical computations mentioned in the Introduction. Though experimental observations bearing on velocity adjustments are sparse, the results of *Schowalter* and *Allen* (15) for non-Newtonian jets and the results of *Gottlieb* and *Bird* (3) for non-Newtonian and Newtonian jets do appear to exhibit such dynamics. The measurements of *Gottlieb* and *Bird* were conducted at fairly small Reynolds numbers and in their figure 5 (the smallest $Re = 4.94 \cdot 10^{-2}$ in their experiments) they observed the same profiles qualitatively as those shown in our figure 2a, but with less velocity adjustment in the exit region. Their maximum velocity at $x = 0$ is about 8% larger than that obtained from our calculations and their velocity profile does not seem to exhibit a stress singularity at the exit lip.

In general, we expect the solutions of this paper to exaggerate the effects of the singularity, the swell and other functionals of the solution in the sense that terms of neglected order will moderate effects predicted at lower orders. This belief has no rigorous justification other than experience with other problems. However, *Silliman* and *Scriven* (16) did compare the swell in a plane jet computed by them using finite elements with the swell computed analytically by *Richardson*. The agreement was good for $(\mu\bar{U})/\sigma < .1$ and not bad for $(\mu\bar{U}/\sigma < 1.$. In all cases *Richardson's* formula [4.10] *overestimates* the computed swell. The same can be expected to hold relative to our [4.9].

It is probable that the graphs shown in the figures of this paper are an exaggerated representation of trends characteristic of actual low speed jets.

Appendix I: Convergence of H_f and ϕ for large n

$$H_f = -2\sum_{1}^{\infty} a_n J_0(q_n),$$

$$a_n = \frac{q_n[q_n A_n + 2(b_n - B_n)]}{1 + q_n^2},$$

$$b_n = \frac{q_n^2}{1 + q_n^2} B_n.$$

We see that for large n, $b_n \sim B_n$ and hence that $a_n \sim A_n$. Therefore, H_f behaves like $A_n J_0(q_n)$ for large n.

Now

$$A_n = \frac{4i}{J_0(q_n)} \lim_{\omega \to -iq_n} \frac{d}{d\omega}\left[\frac{1}{\omega^2 B_-(\omega)}\right].$$

We know that

$$B_-(\omega) \sim \omega^{-1/2} \quad \text{for} \quad |\omega| \to \infty,$$

$$\Rightarrow \frac{dB_-(\omega)}{d\omega} \sim \omega^{-3/2} \quad \text{for} \quad |\omega| \to \infty,$$

$$\Rightarrow \frac{d}{d\omega}\left[\frac{1}{\omega^2 B_-(\omega)}\right] \sim \omega^{-5/2} \quad \text{for} \quad |\omega| \to \infty.$$

Thus we see that

$A_n J_0(q_n) \sim q_n^{-5/2}$ for large n,

and since,

$q_n \sim \pi(n + \frac{1}{4})$

we have that,

$H_f \sim (n + \frac{1}{4})^{-5/2}$ for large n.

Turning now to the asymptotic formula for the pressure, we have

$$\phi = -4\sum_{-\infty}^{\infty} C_n J_1^2(p_n) = -8\sum_{1}^{\infty} \mathrm{Re}[C_n J_1^2(p_n)],$$

$$C_n = \frac{4B_+(ip_n)}{p_n J_1^2(p_n)},$$

$$\Rightarrow C_n J_1^2(p_n) = \frac{4B_+(ip_n)}{p_n}.$$

Now, we know that

$$B_+(\omega) \sim \omega^{-1/2} \quad \text{for} \quad |\omega| \to \infty,$$

$$\Rightarrow C_n J_1^2(p_n) \sim \frac{4i^{1/4}}{p_n^{3/2}} = \frac{4e^{i\frac{\pi}{4}}}{p_n^{3/2}}$$

and hence

$$\mathrm{Re}[C_n J_1^2(p_n)] \sim 2\left[\frac{e^{i\frac{\pi}{4}}}{p_n^{3/2}} + \frac{e^{-i\frac{\pi}{4}}}{\bar{p}_n^{3/2}}\right].$$

Then

$$\mathrm{Re}[C_n J_1^2(p_n)] \sim 2\left[\frac{e^{i\frac{\pi}{4}}\bar{p}_n^{3/2} + e^{-i\frac{\pi}{4}}p_n^{3/2}}{p_n^{3/2}\bar{p}_n^{3/2}}\right]$$

$$\sim \frac{\mathrm{Re}[e^{-i\frac{\pi}{4}}p_n^{3/2}]}{|p_n^{3/2}|^2} = \frac{\mathrm{Re}[e^{-i\frac{\pi}{4}}p_n^{3/2}]}{|p_n|^3}.$$

Now both the real and imaginary parts of $p_n \to \infty$ as $n \to \infty$, however the real part is several orders of magnitude larger, so that

$$\frac{\mathrm{Re}[e^{-i\frac{\pi}{4}}p_n^{3/2}]}{|p_n|^3} \sim \frac{\mathrm{Re}[p_n^{3/2}]}{|p_n|^3} \sim \frac{|p_n|^{3/2}}{|p_n|^3},$$

thus,

$$\mathrm{Re}[C_n J_1^2(p_n)] \sim \frac{1}{|p_n|^{3/2}}.$$

We note that

$$|p_n| = (\{\mathrm{Re}[p_n]\}^2 + \{\mathrm{Im}[p_n]\}^2)^{1/2}$$

$$= \mathrm{Re}[p_n]\left(1 + \left\{\frac{\mathrm{Im}[p_n]}{\mathrm{Re}[p_n]}\right\}^2\right)^{1/2},$$

and since $\mathrm{Re}[p_n] \gg \mathrm{Im}[p_n]$ for n large we have that

$$\mathrm{Re}[C_n J_1^2(p_n)] \sim \frac{1}{\mathrm{Re}[p_n]^{3/2}}.$$

Now

$$p_n \sim \left(n + \frac{1}{2}\right)\pi + \frac{i}{2}\log 2\pi(2n+1),$$

therefore $\phi \sim \dfrac{1}{(n+\frac{1}{2})^{3/2}}$ for large n.

Appendix II: Upper and lower bounds for H_f and ϕ

Consider any convergent sum, S, for which the individual terms are known to behave in a particular asymptotic fashion.

$$S = \sum_1^\infty a_n$$

where

$$a_n = \frac{a}{(n+\beta)^p} \quad \text{for large } n, p > 1.$$

Now,

$$S = \sum_1^M a_n + \sum_{M+1}^\infty a_n$$

$$\equiv S_M + R_M,$$

where S_M is a partial sum and R_M the remainder.

Define $f(n) = a_n$.

We seek numbers S_M^L and S_M^U such that

$$S_M^L < S < S_M^U \quad \forall\, M > N.$$

To do this we implement the Cauchy integral test. From the Cauchy integral test we have

$$R_M > \int_{M+1}^\infty f(x)dx$$

and

$$R_M - a_{M+1} < \int_{M+1}^\infty f(x)dx \quad \forall\, M.$$

Thus,

$$S_M + \int_{M+1}^\infty f(x)dx < S < S_{M+1} + \int_{M+1}^\infty f(x)dx \quad \forall\, M. \qquad \text{[II.1]}$$

At this point we reason that $f(x)$ may be replaced with its asymptotic representation and the inequality will still be preserved $\forall\, M > N$. The number N will in general depend upon the nature of convergence and will have to be determined numerically. Substituting the asymptotic formula into [II.1]

$$S_M + \alpha\int_{M+1}^\infty \frac{dx}{(x+\beta)^p} < S < S_{M+1} + \alpha\int_{M+1}^\infty \frac{dx}{(x+\beta)^p} \quad \forall\, M > N,$$

where α is determined by requiring that

$$a_{M+1} = \frac{\alpha}{(M+1+\beta)^p}.$$

Now,

$$\int_{M+1}^\infty \frac{dx}{(x+\beta)^p} = \frac{1}{(p-1)(M+1+\beta)^{p-1}},$$

and thus,

$$\alpha\int_{M+1}^\infty \frac{dx}{(x+\beta)^p} = \frac{a_{M+1}(M+1+\beta)^p}{(p-1)(M+1+\beta)^{p-1}} = \frac{a_{M+1}(M+1+\beta)}{p-1}.$$

Therefore we have that

$$S_M + \frac{a_{M+1}(M+1+\beta)}{p-1} < S < S_{M+1} + \frac{a_{M+1}(M+1+\beta)}{p-1} \quad \forall\, M > N,$$

and thus that

$$S_M^L = S_M + \frac{a_{M+1}(M+1+\beta)}{p-1} \qquad \text{[II.2]}$$

and

$$S_M^U = S_{M+1} + \frac{a_{M+1}(M+1+\beta)}{p-1}.$$

We are interested in partial sums of the series for H_f and ϕ which are given in Appendix I.

For $M > 9$ the upper and lower bounds for H_f (see [II.2], $\beta = 1/4$, $p = 5/2$) were found to respectively decrease and increase monotonically with M. The partial sums after 99 and 100 terms were respectively .49356 and .49357, and the upper and lower bounds for $M = 99$ were the same to 5 decimal digits at .49389. Actually for $M > 79$ the upper and lower bounds remained unchanged to 5 decimal digits at .49389.

The upper and lower bounds for ϕ (see [II.2], $\beta = 1/2$, $p = 3/2$) were found to respectively decrease and increase for $M > 19$. The partial sums after 99 and 100 terms were respectively 3.1479 and 3.1500. For $M = 99$ the upper and lower bounds were found to be respectively 3.5542 and 3.5522.

Acknowledgement

This work was supported by the U.S. Army Research Office and by a grant from the U.S. National Science Foundation.

Summary

The stick-slip problem for a round jet is solved in two ways: by a Wiener-Hopf method and by a direct method in which eigenfunction solutions in the pipe and jet are matched on their common boundary. The same solution is obtained by the two methods, but the eigenfunction method is more direct and converges more rapidly. Reliable graphs are presented for the distributions of the velocity components, stresses and pressures at different axial positions in the pipe and jet. The shape of the free surface for the low speed jet is computed by a perturbation method.

Zusammenfassung

Das Haft-Gleit-Problem wird für einen runden Strahl auf zwei verschiedene Weisen gelöst: durch die Wiener-Hopf-Methode und durch eine direkte Methode, bei der die Eigenfunktionslösungen für Rohr und Freistrahl an der gemeinsamen Grenze aneinander angeschlossen werden. Mit beiden Methoden erhält man die gleiche Lösung, aber die Eigenfunktionsmethode ist direkter und konvergiert schneller. Glaubwürdige graphische Darstellungen des Verlaufs der Geschwindigkeitskomponenten, der Spannungen und der Drücke für verschiedene axiale Lagen in Rohr und Freistrahl werden mitgeteilt. Die Gestalt der freien Oberfläche für einen mit langsamer Geschwindigkeit austretenden Strahl wird mit Hilfe einer Störungsmethode berechnet.

References

1) *Abramowitz* and *Stegun,* Handbook of Mathematical Functions (Dover 1970).

2) *Chang, P. W., T. W. Patten, B. A. Finlayson,* Computers and Fluids **7**, 285–293 (1979).

3) *Gottlieb, M., R. B. Bird,* I & EC Fundamentals **18**, 357–368 (1979).

4) *Gregory, R. D.,* The Semi-infinite strip $x \geq 0$, $-1 \leq y \leq 1$; Completeness of the Papkovich-Fadle Eigenfunctions when $\phi_{xx}(0,y)$, $\phi_{yy}(0,y)$ are prescribed. Tech. Report No. 78–37, The Inst. of Appl. Math. and Statistics, the Univ. of British Columbia, Vancouver, Canada (1978).

5) *Gregory, R. D.,* The Traction Boundary-value Problem for the Elastostatic Semi-infinite Strip; Existence of Solution and Completeness of the Papkovich-Fadle Eigenfunctions. Tech. Report No. 79 to 23, The Inst. of Appl. Math. and Statistics, the Univ. of British Columbia, Vancouver, Canada (1979).

6) *Gregory, R. D.,* J. Elasticity **9**, 1–27 (1979).

7) *Jean, M., W. G. Pritchard,* The Flow of Fluids from Nozzles at Small Reynolds Numbers. To appear in Proc. of Royal Society, London, A (1980).

8) *Joseph, D. D.,* Arch. Rational Mech. Anal. **56**, 99–157 (1974).

9) *Joseph, D. D.,* A new Separation of Variables Theory for Problems of Stokes Flow and Elasticity. "Trends in Applications of Pure Mathematics to Mechanics", vol. II (Proceedings of a Symposium at Kozubnik, Poland in Sept. 1977, H. Zorski, ed.) Pitman (London 1979).

10) *Michael, D. H.,* Mathematika **5**, 82–84 (1958).

11) *Nickell, R. E., R. I. Tanner, B. Caswell,* J. Fluid Mech. **65**, 189–206 (1974).

12) *Noble, B.,* Methods based on the Wiener-Hopf technique, Pergamon Press (1958).

13) *Omodei, B. J.,* Comp. Fluids **7**, 79–96 (1979).

14) *Richardson, S.,* Proc. Comb. Phil Soc. **67**, 477–489 (1970).

15) *Schowalter, W. R., R. C. Allen,* Trans. Soc. Rheol. **19**, 129–137 (1975).

16) *Silliman, W. J., L. E. Scriven,* J. Computational Phys. **34**, 287–313 (1980).

17) *Sturges, L. D.,* Ph. D. thesis, University of Minnesota (1977).

18) *Tanner, R. I., K. R. Reddy,* Finite Element Method for the Solution of some Non-Newtonian Fluid Mechanics Problems; in: Y. K. Cheung and S. G. Hutton (eds.), "Finite Element Methods in Engineering", Univ. of Adalaide (1976).

19) *Titchmarsh, E. C.,* The theory of Fourier integrals, Oxford Univ. Press (1962).

20) *Trogdon, S. A.,* Ph. D. thesis, University of Minnesota (1980).

21) *Zidan, M.,* Rheol. Acta **8**, 89–123 (1969).

Authors' addresses:

Prof. *D. D. Joseph*
Department of Aerospace Engineering
and Mechanics
University of Minnesota
Minneapolis, Minnesota 55455 (USA)

Dr. *S. A. Trogdon*
Department of Mechanical
and Industrial Engineering
Clarkson College of Technology
Potsdam, New York 13676 (USA)